Materials Views
www.MaterialsViews.com

ADVANCED FUNCTIONAL MATERIALS
www.afm-journal.de

A New Material for High-Temperature Lead-Free Actuators

*Ahmed Kursumovic, Emmanuel Defay, Oon Jew Lee, Chen-Fong Tsai, Zhenxing Bi, Haiyan Wang, and Judith L. MacManus-Driscoll**

Unimorph cantilevers are made from 0.5BaTiO$_3$-0.5Sm$_2$O$_3$ (BTO-SmO) self-assembled vertical heteroepitaxial nanocomposite thin films, grown by PLD on (001) SrTiO$_3$ single crystal substrates. The films remain piezoelectric up to at least 250 °C without losing any actuation. The longitudinal piezoelectric coefficient, d_{33}, is ≈45 to 50 pm V^{-1} measured from room temperature to 250 °C. The transverse piezoelectric coefficient, d_{31}, a key parameter of actuator performance, exceeds PZT (Pb$_{1-x}$Zr$_x$TiO$_3$) films at >200 pm V^{-1}. Since the d_{31} coefficient was found to be positive, this opens up exciting new applications opportunities. The possible reasons for $d_{31} > 0$ are discussed in the light of 3D strain control in the nanocomposites.

1. Introduction

As part of the drive towards miniaturization of devices of functional materials, piezoelectricity in film form has gained popularity, particularly in the areas of micro-electromechanical systems (MEMS) and energy harvesters.[1] On the other hand, the best performing materials are based on standard Pb$_{1-x}$Zr$_x$TiO$_3$ (PZT) which contains Pb as a significant constituent. For environmental reasons a Pb-free alternative material is urgently needed.[2,3] The classical BaTiO$_3$ (BTO) material and its derivatives are possible alternatives with relatively high piezoelectric response. However, the rather low Curie temperature, T_c, of BaTiO$_3$ (≈130 °C) means the operation temperature is limited to near room temperature. On the other hand it has been shown that epitaxial BTO films of up to 50 nm thickness can be stabilized to rather high temperatures through T_c enhancement from substrate strain control of the structure.[4] However, owing to their inherent thickness limitation of ≈50 nm, these films are not robust enough for electromechanical related applications. Also, the low volume of material means that the magnitude of the effects are limited. On the other hand, novel vertical heteroepitaxial nanocomposite films of BaTiO$_3$-Sm$_2$O$_3$ (BTO-SmO) can be grown to >1 µm thickness while maintaining high T_c of up to 800 °C, as well as excellent mechanical robustness.[5,6]

The strain in the self-assembled BTO-SmO composite develops in the vertical direction between the BTO matrix and the ≈10 nm SmO pillars which grow embedded in the matrix. This vertical interfacial strain is caused by lattice mismatch between the two phases in the film, rather than from thermal expansion mismatch (brought about by cooling from the deposition temperature) which could be expected to predominate in thicker (>100 nm) BTO films, which are interfaced with the substrate on one side only.[6,7]

Owing to their high T_c, the micrometer thick BaTiO$_3$-Sm$_2$O$_3$ nanocomposite materials have great potential to work as piezoelectrics well above room temperature and hence to drive moderate loads. In this work we explore these piezoelectric properties. We find high longitudinal piezoelectric coefficient d_{33} (>45 pm V^{-1} measured from room temperature to 250 °C) as well as high and positive transverse piezoelectric coefficient d_{31} (>200 pm V^{-1}).

2. Results and Analysis

Figure 1a shows characteristic X-ray diffraction (XRD) traces of three BTO-SmO films (40, 100 and 500 nm thickness) on (001) SrTiO$_3$ (STO) substrates measured at room temperature (RT). Consistent with our earlier studies, the out-of-plane lattice parameter of the BTO was found (100 nm film in Figure 1a) to be in tension by ≈1% compared to bulk BTO (c = 0.40593 nm compared to 0.40343 nm in bulk BTO).[7] As we discussed in an earlier report, from measured out-of-planes lattice parameters, it was found that $2\times (001)_{\text{BTO-strained-comp.}}$ (= 2 × 0.40593 nm = 0.81186 nm) ≈ $3 \times (004)_{\text{SmO-strained-comp}}$ (= 3 × 1.0928/4 nm = 0.8196 nm).[6] Hence, along the vertical interface, there is 2:3 domain matching epitaxy which controls the amount of out-of-plane strain. The vertical mismatch amounts to about 1%. In this work, it was found that different thicknesses affect the

---

Dr. A. Kursumovic, Dr. O. J. Lee,
Prof. J. L. MacManus-Driscoll
Cambridge University
Department of Materials Science
Pembroke St., Cambridge, CB2 3QZ, UK
E-mail: jld35@cam.ac.uk
Dr. E. Defay
CEA-LETI, Minatec Campus
17 Rue des Martyrs, 38054 Grenoble, France
C.-F. Tsai
Materials Science and Engineering Program
Texas A&M University
College Station, TX 77843, USA
Dr. Z. Bi, Prof. H. Wang
Department of Electrical and Computer Engineering
Texas A&M University
College Station, TX 77843, USA

DOI: 10.1002/adfm.201300899

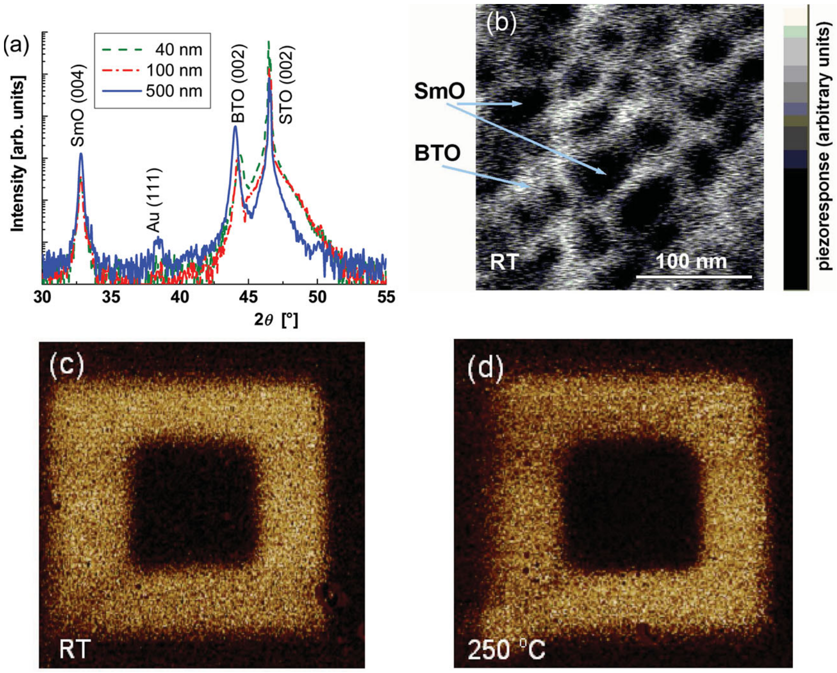

Figure 1. a) XRD scans of some of the composite films used in this work (40, 100 and 500 nm thick). b) RT PFM amplitude scan (V_{DC} = 10 V, V_{AC} = 2 V, f = 15 kHz) of a 100 nm thick film. c) RT PFM phase contrast scan on 40 nm thick BTO-SmO film after –10 V writing (2.5 μm^2), +10 V rewriting (1.5 μm^2) and –10 V rewriting (0.75 μm^2). d) Same as (c) but at 250 °C.

level of BTO strain, as would be expected since for thicker films the substrate plays less of a role in controlling the strain. Note that the vertical mismatch/strain with respect to the high temperature cubic phase is much larger (≈2.5%), ensuring the tetragonal lattice is stabilized from the deposition temperature of ≈800 °C.[4–6]

We must also consider effects arising from the mismatch of the thermal expansion coefficients. From our previous work it was established that the *c*-axis thermal expansion coefficient of the BTO phase is about 12×10^{-6} for a 150 nm film, $\approx 10.8 \times 10^{-6}$ for a 600 nm film, 9×10^{-6} for SmO bulk, and 11×10^{-6} for STO substrate.[6] This would produce a thermal expansion induced mismatch for 150 and 600 nm films, of around 0.15% to 0.25%, respectively, when the sample is cooled from the deposition temperature of 800 °C to room temperature. This mismatch is considerably smaller than estimated (≈1%). However, evidence to show that lattice mismatch plays a dominant role is that the samples are cooled from the deposition temperature down to room temperature in the tetragonal (and not cubic) phase.[6] The lattice strain observed matches the theoretical predictions of the T_c increase that we observed.[5]

The film in-plane orientation was found to be $\langle 100\rangle_{BTO} \parallel \langle 100\rangle_{STO}$ and for the SmO $\langle 100\rangle_{SmO} \parallel \langle 110\rangle_{STO}$.[6] The in-plane lattice parameter of the BTO measured from reciprocal space maps of the (113) peak (not shown) indicated values of ≈0.40305 nm corresponding also to an in-plane tension of ≈1%. This unexpected auxetic-like behavior is discussed later in the context of results of the piezoelectric measurements in the presence of a three dimensional (3D) strain state in the BTO matrix brought about by the stiff SmO nanocolumns and STO substrate.[8,9]

A piezo-force-microscopy (PFM) image on a small scale (250 nm × 250 nm, Figure 1b) confirms the presence of two phases in the vertical composite arrangement. Only the BTO matrix shows piezo-related activity (brighter region) while the SmO nanopillars do not (darker regions), indicating strong piezoelectricity of the matrix and apparent rigidity of the nanopillars in the BTO-SmO composite film. The PFM scans were performed at a frequency, f, of 15 KHz with an alternating current (AC) voltage $V_{AC} = 2V\sin(2\pi f)$ while being polarized by a direct current (DC) bias of V_{DC} = 10 V.

It was possible to write on the films up to 100 nm in thickness by a PFM tip with a ±10 V writing signal using a conductive PFM tip (Figure 1c). The phase contrast was maintained for several days (the longest time studied) proving the ferroelectric nature of the composite films. The maximum temperature studied was about 250 °C (Figure 1d), the limit of the instrument (PFM sample heater) and stability of the PFM cantilevers used.

Characteristic butterfly loops were obtained with PFM spectroscopic measurements, while sweeping the DC voltage from +10 to –10 to +10 V and measuring the piezoresponse to a small AC voltage at frequency f = 15 kHz, from which $d_{33} \approx$ 45 to 50 pm V^{-1} was obtained (**Figure** 2a), indicating again strong piezoelectricity in the BTO-SmO composite film. The horizontal shift in the coercive field is believed to be due to the different electrodes used (Pt tip and Nb-doped STO), as well as from the built in BTO-SmO strain. The d_{33} value obtained is much higher than the recent literature data of ≈20 pm V^{-1} for pure BTO thin films.[10] On the other hand, it is consistent with the high vertical tensile

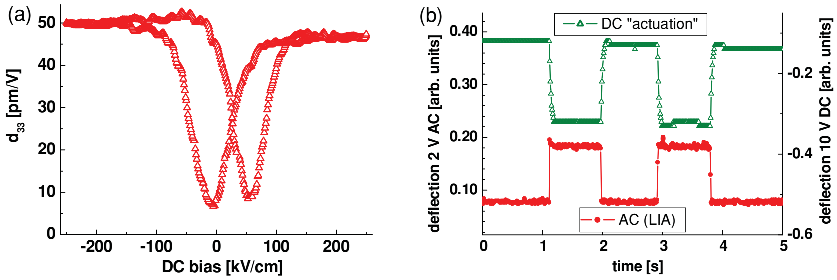

Figure 2. Measurements of piezoelectric coefficients at 250 °C in 40 nm BTO/SmO films deposited on 0.5 mm thick Nb-doped STO STO. a) d_{33} from standard PFM spectroscopy, applying V_{ac} = 2 V at f = 15 kHz. b) Unimorph cantilever deflection $\delta \propto d_{31}$ measured at L = 2.5 mm from the fixing point (see Experimental Section), induced by step polarization (10 V DC off/on/off/on/off) V_{ac} = 2 V and f = 500 Hz. Note that the DC-induced deflection is negative.

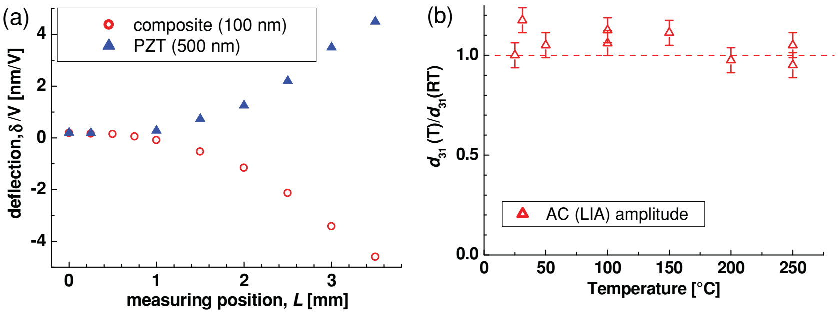

Figure 3. Calculated d_{31} values, from actuator deflection measurements. a) RT static deflection (for 40 V DC bias) in 100 nm BTO/SmO film compared to 500 nm thick PZT film, both on 0.5 mm thick STO "beams". b) d_{31} of the BTO-SmO composite, measured up to 250 °C, normalized by its room temperature value; LIA response is for a 2 V AC (500 Hz) drive; the error bars are at the <±10% level and are estimated from >5 measurements per point.

strain effect (and conconomitant T_c increase) produced in the matrix of the composite structure.[6] However, the apparent d_{33} value is still below ≈100 pm V^{-1} for a single-crystal BaTiO$_3$, which is likely due to both clamping and the microstructural defects usually present in thin films.[8,11,12]

The cantilever d_{31} properties were determined, simultaneously from the step-like DC (V_{DC} on/off) and low frequency AC voltage measurements of a unimorph cantilever beam made of 100 nm BTO-SmO film on 0.5 mm STO substrate. Both signals AC from the lock-in amplifier (LIA, that controls and measures cantilever vibration) and the DC output from the split-diode were monitored (Figure 2b). The DC related movement was also monitored by the Z-axis servo of the piezo-scanner movement when in the constant force mode. The DC actuation (Figure 2b) is prone to thermal drift and eventual heating fluctuations (self-heating and the "furnace" instability), hence the measurements were done in a rather short time of 0.1 to 1 s.

The results of the room temperature deflection measured at different lengths along the cantilevers of BTO/SmO on STO, compared to PZT on STO, are shown in **Figure 3**a. The deflections were well approximated with the second order polynomial (quadratic function of L) as predicted in Equation (1), shown later. The results, for DC actuation, shown here do not include any of the atomic force microscopy (AFM) cantilever slope contribution, since they were taken from the constant-force AFM-PFM measurements. The calculated transverse piezoresponse coefficient d_{31} was between +200 and +300 pm V^{-1}. This uncertainty is due to not precisely knowing the in-plane elastic properties of the film. However, the d_{31} induced deflection (δ) obtained was comparable or better than δ of the PZT film. The opposite sign of the cantilever response of non-polarized PZT/STO films unambiguously proves the positive d_{31} sign of the composite. The possible reasons for the positive d_{31} are included in the Discussion section.

The magnitude of the actuation measured at RT for the nanocomposite films is high and is similar to PZT (Figure 3a) and lead-free competitor materials, namely strained (Na,Bi)TiO$_3$–BaTiO$_3$ epitaxial thin films on (110) MgO, with T_c up to 200 °C, that have large RT d_{31} values of 210 pm V^{-1} rivaling the properties of epitaxial PZT films.[3,13–16] Some doped PZT films still have high Curie temperature ($T_c \approx 600$ °C) and high RT d_{31} but no high d_{31} has been reported at elevated temperatures.[17]

Attempts have been made to improve T_c of Pb-free piezoelectrics such as promising (Ba,Ca)(Ti,Zr)O$_3$ by doping with high T_c (but low d_{33} and d_{31}) BiFeO$_3$. However, albeit slight improvements in d_{33} (for light doping) the T_c was reduced, presumably due to Bi substitution for Ba^{2+} site.[18]

However, there are, to the best of our knowledge, no above room temperature reports of d_{31} values on Pb-free piezoelectric materials, but their relatively low Curie temperature values (below 400 °C, as compared to ≈800 °C in BTO-SmO films) likely indicate that they do not possess d_{31} retention to high temperatures.[6] Hence, the main advantage of the composite films of this study, in addition to simple composition, high reproducibility of properties and low leakage is the high temperature retention of a high piezoresponse.[6]

In our composite films actuation δ and hence d_{31} showed little dependence on the temperature up to a maximum measurable of 250 °C, as shown in Figure 3b. This is very promising for high temperature microactuators and energy harvesting applications.

3. Discussion

We consider the reasons for the magnitudes and signs of the piezoelectric coefficients, d_{33} and d_{31} measured in our nanocomposite cantilever structures.

The high d_{33} value (>45 pm V^{-1}) obtained at room temperature is above that for typical, pure BTO films (of <30 pm V^{-1}) and is understandable because the vertical tensile strain of ≈1% increases the displacement of the Ti ion along the c-direction (or effectively adds to the polarization voltage).[10] It is also possible that the increased d_{33} measured arises in part from structural softening along the interface regions with SmO (due to effectively reduced elastic constants in the interfacial region, thus reducing the clamping).[12]

It should be pointed out that in most of the piezoelectric materials, d_{33} is roughly twice as large as d_{31} and they are of opposite signs. Here the fact that d_{31} is so large and that it exhibits the same sign as d_{33} suggests that another phenomenon is induced. The variation of the BTO Young's modulus could be involved in this process as this would induce a stress balance variation between the BTO matrix and SmO pillars. This variation could be related to the unusual 3D strain state in the vertical heteroepitaxial nanocomposites, rather than any small composition changes in the BTO which, in fact, we have found to be very minimal.[6,8]

Very thin films, i.e., 40 to 100 nm BTO-SmO on STO, still "feel" some of the influence of substrate strain. This semi-3D stress strain produces an auxetic-like situation which is more pronounced in thinner films. If one assumes relaxation across the substrate-film interface, at the deposition temperature, when the film cools down SmO gets partly stretched horizontally (due to a negative thermal mismatch with the substrate) offsetting the vertical expansion caused by SmO mismatch/

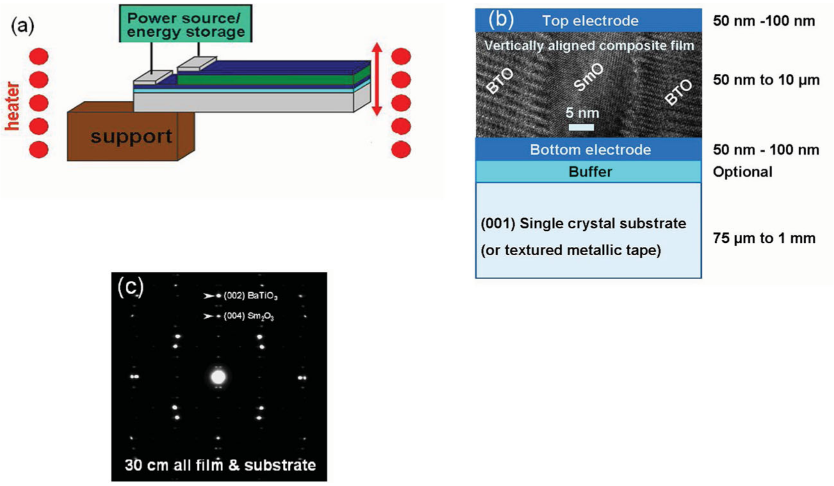

Figure 4. Details of the cantilever structure studied. a) Schematics of the unimorph cantilever. b) Cross-section detail with the HRTEM image inserted. c) Selected area diffraction (SAD) patterns obtained in the TEM for film and substrate show highly epitaxial nanocomposite growth. The orientation relationships are determined to be BTO(002)||SmO(004)||STO(002) and BTO(020)||SmO(220)||STO(020).

strain/stress. This effect disappears as the films get much thicker. The apparent anomaly of the BTO XRD peak being more shifted towards lower angles as the samples get thinner (but not for SmO) is in accordance with the observed behavior in bulk composites for strains below about 1%, where the iso-stress Reuss model was found to apply.[19] There fibers deform uniformly but much less so than the matrix. However, at larger strains (>1%) the Voigt type behavior can be expected. On the other hand, the SmO nanopillars (which are much stiffer than the BTO matrix) are strained much less than the BTO. Hence, the SmO (004) peak does not shift significantly. This effect was discussed earlier in.[6]

For BTO, the increased *c* lattice parameter corresponds to a ≈1% tensile strain and arises from the surrounding, stiff SmO (Young's modulus $E_{\mathrm{SmO}} \sim 125$ GPa >> $E_{\mathrm{BTO}} \sim 65$ GPa) nanopillars which act like "reinforcement" rods in the films.[6] The pitch of the rods (Figure 1b) is ≈30 to 40 nm, i.e. <2× their diameter, leaving "rings" of BTO surrounding them of <20 nm thickness, which means that all the BTO is subject to stress from the reinforcement rods. From the measured positive (tensile) strains both out-of-plane and in-plane, as well as the concomitant positive d_{31} and d_{33} values, it appears that the 3D stress state is very effective in the films. Hence, the strain appears not to be only vertical and uniaxial as we postulated previously but quasi-hydrostatic, with epitaxy playing strong roles both laterally and vertically.[6] As a result of the positive d_{31} the stretched cantilever exhibits transverse expansions, rather than contraction as would normally be the case of a piezoelectric unimorph exhibiting Poisson's elastic behavior. A similar behavior had been observed previously in both $BaTiO_3$-$CoFe_2O_4$ and $BiFeO_3$-$CoFe_2O_4$ although those effects were believed to result from defects and intermixing, i.e. non-stochiometry and composition change.[20,21]

Finally, we consider the practical consequences of the high and positive values of both d_{33} and d_{31}, coupled with high temperature operation of the piezoelectric unimorph structures (no measureable degradation up to 250 °C in our chemically benign, Pb-free material). The system is a very promising alternative to PZT in microactuation and energy harvesting applications, including in MEMS applications where films of thickness of a few hundred nm up to couple of hundred μm are used (see ref. [22] for a review). The high positive d_{31} values could lead to a very large hydrostatic piezoelectric coefficient, thus opening the door for using our composite film structures for transmitters and receivers as well as ultrasonic power sensors in medical imaging. The next step is in situ integration on Si wafers, and this is highly possible since it has already been shown that highly epitaxial $SrRuO_3$ can be grown on Si (001).[23]

4. Conclusions

Self-assembled, lead free unimorph cantilever films of $0.5BaTiO_3$-$0.5Sm_2O_3$ (BTO-SmO) were grown by pulsed laser deposition on single crystal substrates. The films grow with vertical SmO nanopillars embedded in a $BaTiO_3$ matrix which is highly strained by the pillars. The d_{33} values are higher than pure BTO films, >45 pm V^{-1} measured from room temperature to 250 °C. These high values arise from the high out-of-plane vertical strain induced by the SmO on the BTO which also increases T_c. Surprisingly the d_{31} values are positive and large (200 to 300 pm V^{-1}) and the possible reasons for this apparent auxetic effect are discussed. Finally, the unimorphs function without degradation of piezoelectric properties or physical robustness up to 250 °C, the highest temperature studied. They also perform better than PZT unimorphs (at RT) studied here. The nanocomposite thin film system has great potential to replace PZT in microactuator and microenergy harvesting applications.

5. Experimental Section

Experimental Set Up: BTO-SmO films were grown by pulsed laser deposition (excimer laser of wavelength 248 nm) from a composite target made in-house from pure (>4 N) $BaTiO_3$ and Sm_2O_3 powders in 50:50 volume ratio. The films were deposited onto conductive (100) Nb-doped STO substrates. The BTO-SmO composite films were grown to thicknesses from 40 to 500 nm at 800 °C under 0.15 Torr (≈0.02 mbar) $p(O_2)$. For d_{31} measurements, top Pt or Au electrodes (<50 nm thick, covering 90% of the film) were deposited by RF sputtering at RT. A reference $Pb_{0.99}(Zr_{0.45}Ti_{0.47}(Ni_{0.33}Sb_{0.67})_{0.88})O_3$ (PZT) film of ≈500 nm thickness was deposited by PLD using a PZT commercial target at ≈700 °C in pure oxygen under 0.15 Torr (≈0.2 mbar) $p(O_2)$ also onto (100) Nb-doped STO substrate.[24]

Films were characterized using XRD for out-of-plane crystallinity as a measure of the texture and strain. Cross-sectional images of the film were undertaken with high resolution transmission electron microscopy (HRTEM) performed on a JEOL 2011FEG/JEOL 4000EX/Philips CM30 microscope.

Piezoresponse measurements were carried using an Agilent 5500 Scanning Probe Microscope (SPM) equipped with three (MAC-3) lock-in amplifiers (LIAs). Measurements were performed from RT up to 250 °C

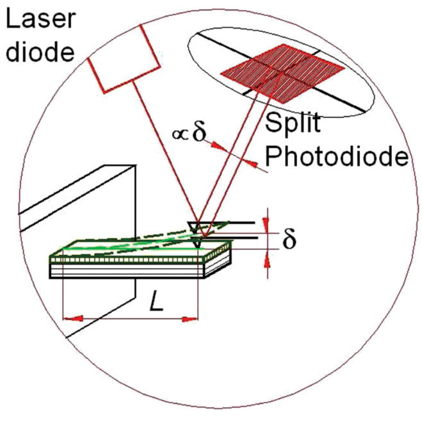

Figure 5. Schematics of deflection δ, at position L, measurements by an AFM cantilever.

(**Figure 4**a). The piezoresponse signals were calibrated using a standard height (Micro-Mesh) sample and the $LiNbO_3$ PFM factory standard sample (Bruker) with $d_{33} = 7.5$ pm V^{-1}.

d_{33} and d_{31} Calculations: Standard PFM experiments were performed for the d_{33} measurements of a bare BTO-SmO film with a conductive Nb-doped STO substrate as the bottom electrode. Conductive AFM cantilevers of 75 kHz self-resonance were used with Pt or doped-DLC (diamond like carbon) coated tips. The PFM voltage was applied to the cantilever tip or the bottom electrode while in the contact mode. A DC voltage up to ±40 V was used for bias (polarization), while AC voltage $V = V_{ac}\cos(2\pi ft)$ up to $V_{ac} = 5$ V was applied. The frequency (f) ranged from 200 Hz to 15 kHz, well below the 75 kHz resonance. In the saturated (DC) regime, the measured local longitudinal displacement $z = d_{33} \times V_{ac}$ was used to calculate the coefficient d_{33}, while the actual d_{33} butterfly figure (Figure 2a) was obtained by correcting the amplitude for the LIA's phase response. However, deposited (clamped) films to a rigid substrate do not show real but an effective d_{33} coefficient, which is affected by the elastic compliances and d_{31} coefficient of the film. Resulting d_{33} values are normally lower than in the corresponding bulk.[12] Furthermore, effective d_{33} values are dependent on the extent of the substrate rigidity.[25–27]

Non-standard PFM measurements were performed in order to estimate the d_{31} coefficient of the films. For this purpose, the samples were formed into composite cantilever structures by mounting (mechanical clamping) at one end (Figure 4a,b). The structure was relatively thin and narrow with respect to the length. A voltage was applied between top and the bottom electrode (Figure 4b) to induce longitudinal and transverse displacements of the whole sample. Again, an Agilent 5500 SPM was used but the conductive AFM cantilever used in constant force mode, was at the same (ground) potential as the top metal electrode in order to eliminate electrostatic bending and the errors involved.[28] The AFM cantilever was positioned at different lengths L from the end support/clamp (**Figure 5**) of our composite cantilever for respective d_{31} estimation via measurements of deflection δ. A DC voltage up to ± 40 V (for polarization, and DC part of δ) in combination with AC voltage up to 5 V (for the AC part of δ) was applied to the sample. The AC frequency used ranged from 200 Hz (minimum for the lock-in amplifier) to 500 Hz, well below the composite cantilever resonance which was above 1 kHz.

In here we concentrate especially on the transverse, d_{31}, coefficient as a key value for MEMS type actuators and energy harvesters. Normally d_{33} is defined as positive, hence elongation along the longitudinal direction (c-axis here) is expected to induce transversal contraction and vice-versa. Hence, an in-plane contraction or extension of a piezoelectric film bonded to an elastic cantilever (a bimetallic-type composite structure) would result in the bending of the beam (Figure 5) where the induced free end actuation δ is measured. This δ is proportional to both the applied voltage and d_{31} coefficient, while depends on geometry and elastic constants of the film and the substrate in a complex manner.[29] For our case, where the film is much thinner than the substrate ($t_f << t_s$)[30–32] and the electrode/film covers the whole active area, a simple formula is valid:

$$d_{31} = -\frac{t_S^2}{3L^2}\frac{E_S}{E_f}\frac{\delta}{V} \tag{1}$$

where L is the distance from the anchoring point, E_f and E_s, are Young's moduli of the substrate and the film respectively and t_s is thicknesses of the substrate. In the d_{31} calculations, the Young's modulus of the substrate (Nb doped bulk STO) is $E_s = 238$ GPa.[33] Equation (1) is applicable for all samples studied in this work. Note, however, that maximum δ and the force achieved with such a cantilever are for film and substrate of comparable thickness and comparable elastic constant.

For unidirectional composites, the value of Young's modulus in composite films is usually estimated from a simple rule of mixtures either for Voigt (iso-strain; along the fibers, ‖) or Reuss (iso-stress; perpendicular to the fibers, ⊥) model as:

$$E_{\parallel} = f E_{\mathrm{SmO}} + (1-f) E_{\mathrm{BTO}} \tag{2}$$

and

$$E_{\perp} = \frac{E_{\mathrm{SmO}} E_{\mathrm{BTO}}}{f E_{\mathrm{BTO}} + (1-f) E_{\mathrm{SmO}}} \tag{3}$$

where f is the volume fraction of the fibers (nano-pillars). In our case, for $f = 0.5$, $E_{BTO} \approx 65$ GPa and $E_{SmO} \approx 125$ GPa, this ranges from $E_{\perp} = 85$ to $E_{\parallel} = 95$ GPa. We found the 85 GPa value to be more appropriate as the films, in the thicknesses range studied, behaved more like a Reuss composite. However, the d_{31} results reported ($d_{31} \approx 200$ to 300 pmV^{-1}) included the whole range from a conservative 200 pmV^{-1} to an optimistic 300 pmV^{-1}.

Acknowledgements

This work was supported by the European Research Council (ERC) Advanced Investigator grant (ERC-2009-AdG-247276-NOVOX). The TEM work at Texas A&M University was funded by the U.S. National Science Foundation (NSF 1007969). The authors thank Dr. S. A. Harrington for the 40 nm sample preparation.

Received: March 12, 2013
Revised: April 20, 2013

---

[1] P. Muralt, R. G. Polcawich, S. Trolier-McKinstry, *MRS Bull.* **2009**, *34*, 658.
[2] D. Damjanovic, N. Klein, J. Li, V. Porokhonskyy, *Funct. Mater. Lett.* **2010**, *3*, 5.
[3] C. W. Ahn, S. S. Won, A. Ullah, S. Y. Lee, S. D. Lee, J. H. Lee, W. Jo, I. W. Kim, *Curr. Appl. Phys.* **2012**, *12*, 903.
[4] K. J. Choi, M. Biegalski, Y. L. Li, A. Sharan, J. Schubert, R. Uecker, P. Reiche, Y. B. Chen, X. Q. Pan, V. Gopalan, L.-Q. Chen, D. G. Schlom, C. B. Eom, *Science* **2004**, *306*, 1005.
[5] J. L. MacManus-Driscoll, *Adv. Funct. Mater.* **2010**, *20*, 2035.
[6] S. A. Harrington, J. Zhai, S. Denev, V. Gopalan, H.Wang, Z. Bi, S. A. T. Redfern, S.-H. Baek, C. W. Bark, C.-B. Eom, Q. Jia, M. E. Vickers, J. L. MacManus-Driscoll, *Nat. Nanotechnol.* **2011**, *6*, 491.
[7] G. Vasta, T. J. Jackson, A. Frommhold, J. Bowen, E. J. Tarte, *J. Electroceram.* **2011**, *27*, 176.

[8] H. Zheng, J. Wang, S. E. Lofland, Z. Ma, L. Mohaddes-Ardabili, T. Zhao, L. Salamanca-Riba, S. R. Shinde, S. B. Ogale, F. Bai, D. Viehland, Y. Jia, D. G. Schlom, M. Wuttig, A. Roytburd, R. Ramesh, *Science* **2004**, *303*, 661.

[9] J. L. MacManus-Driscoll, P. Zerrer, H. Wang, H. Yang, J. Yoon, A. Fouchet, R. Yu, M. G. Blamire, Q. X. Jia, *Nat. Mater.* **2008**, *7*, 314.

[10] T. Ohno, K. Uchida, N. Sakamoto, D. Fu, N. Wakiya, T. Matsuda, H. Suzuki, *Jpn. J. Appl. Phys.* **2010**, *49*, 09MA11.

[11] K. Lefki, G. J. M. Dormans, *J. Appl. Phys.* **1994**, *76*, 1764.

[12] A. L. Roytburd, S. P. Alpay, V. Nagarajan, C. S. Ganpule, S. Aggarwal, E. D. Williams, R. Ramesh, *Phys. Rev. Lett.* **2000**, *85*, 190.

[13] H. Adachi, Y. Tanaka, T. Harigai, M. Ueda, E. Fujii, *Appl. Phys. Express* **2011**, *4*, 051501.

[14] Y. Tanaka, T. Harigai, M. Ueda, H. Adachi, E. Fujii, *J. Am. Ceram. Soc.* **2012**, *95*, 3547.

[15] E. Fujii, R. Takayama, K. Nomura, A. Murata, T. Hirasawa, A. Tomozawa, S. Fujii, T. Kamada, H. Torii, *IEEE Trans. Ultrason. Ferroelectr. Freq. Control* **2007**, *54*, 2431.

[16] P. Muralt, *J. Am. Ceram. Soc.* **2008**, *91*, 1385.

[17] C. Zhong, L. Guo, X. Wang, L. Li, *J. Am. Ceram. Soc.* **2012**, *95*, 473.

[18] J. Wu, W. Wu, D. Xiao, J. Wang, Z. Yang, Z. Peng, Q. Chen, J. Zhu, *Current Appl. Phys.* **2012**, *12*, 534.

[19] C. Galiotis, R. J. Young, P. H. J. Yeung, D. N. Batchelder, *J. Mater. Sci.* **1984**, *19*, 3640.

[20] I. Fina, N. Dix, L. Fàbrega, F. Sánchez, J. Fontcuberta, *J. Appl. Phys.* **2010**, *108*, 034108.

[21] a) N. Dix, R. Muralidharan, J. Guyonnet, B. Warot-Fonrose, M. Varela, P. Paruch, F. Sánchez, J. Fontcuberta, *Appl. Phys. Lett.* **2009**, *95*, 062907; b) N. Dix, R. Muralidharan, J. Guyonnet, B. Warot-Fonrose, M. Varela, P. Paruch, F. Sánchez, J. Fontcuberta, *Appl. Phys. Lett.* **2010**, *96*, 076102.

[22] S. Corkovic, Ph.D. Thesis, Cranfield University UK **2007**.

[23] J. Roldan, F. Sanchez, V. Trtik, C. Guerrero, F. Benitez, C. Ferrater, M. Varela, *Appl. Surf. Sci.* **2000**, *154*, 159.

[24] W. Jo, R. Dittmer, M. Acosta, J. Zang, C. Groh, E. Sapper, K. Wang, J. Rödel, *J. Electroceram.* **2012**, *29*, 71.

[25] L. Chen, J. H. Li, J. Slutsker, J. Ouyang, A. L. Roytburd, *J. Mater. Res.* **2004**, *19*, 2853.

[26] Z. Wang, J. Miao, *J. Phys. D: Appl. Phys.* **2008**, *41*, 035306.

[27] Z. Huang, G. Leighton, R. Wright, F. Duval, H. C. Chung, P. Kirby, R. W. Whatmore, *Sens. Actuators A* **2007**, *135*, 660.

[28] B. D. Huey, C. Ramanujan, M. Bobji, J. Blendell, G. White, R. Szoszkiewicz, A. Kulik, *J. Electroceram.* **2004**, *13*, 287.

[29] M. R. Steel, F. Harrison, P. G. Harper, *J. Phys. D: Appl. Phys.* **1978**, *11*, 979.

[30] a) A. L. Kholkin, C. Wutchrich, D. V. Taylor, N. Setter, *Rev. Sci. Instrum.* **1996**, *67*, 1935; b) A. L. Kholkin, M. L. Calzada, P. Ramos, J. Mendiola, N. Setter, *Appl. Phys. Lett.* **1996**, *69*, 3602.

[31] I. Kanno, H. Kotera K. Wasa, *Sens. Actuators A* **2003**, *107*, 68.

[32] H. Imai, I. Kanno, R. Yokokawa, K. Wasa, H. Kotera, *Jpn. J. Appl. Phys.* **2010**, *49*, 09MA11.

[33] P. Paufler, B. Bergk, M. Reibold, A. Belger, N. Pätzke, D. C. Meyer, *Solid State Sci.* **2006**, *8*, 782.